Atmos. Chem. Phys. Discuss., https://doi.org/10.5194/acp-2017-977
Manuscript under review for journal Atmos. Chem. Phys.
Discussion started: 6 November 2017
© Author(s) 2017. CC BY 4.0 License.

Atmospheric Chemistry and Physics Discussions

Isotopic constraints on heterogeneous sulfateproduction in Beijing haze

Pengzhen He[1], Becky Alexander[2], Lei Geng[1], Xiyuan Chi[1], Shidong Fan[1], Haicong Zhan[1], Hui Kang[1], Guangjie Zheng[3]†, Yafang Cheng[3,4], Hang Su[4,3],Cheng Liu[1,5,6],Zhouqing Xie[1,5,6]*

[1]Anhui Province Key Laboratory of Polar Environment and Global Change, School of Earth and Space Sciences, University of Science and Technology of China, Hefei, Anhui 230026, China.

[2]Department of Atmospheric Sciences, University of Washington, Seattle, WA 98195, USA.

[3]Multiphase Chemistry Department, Max Planck Institute for Chemistry, Mainz 55128, Germany.

[4]Jinan University, Institute for Environment and Climate Research, Guangzhou, Guangdong 511443, China.

[5]Key Lab of Environmental Optics and Technology, Anhui Institute of Optics and Fine Mechanics, Chinese Academy of Sciences, Hefei, Anhui 230031, China.

[6]Center for Excellence in Urban Atmospheric Environment, Institute of Urban Environment, Chinese Academy of Sciences, Xiamen, Fujian 361021, China.

**Corresponding to*: Zhouqing Xie (zqxie@ustc.edu.cn)

†: Now at: Atmospheric Sciences Division, Brookhaven National Laboratory, Upton, NY 11973, USA.

Abstract. Discerning mechanisms of sulfate formation during fine-particle pollution (referred to as haze hereafter)in Beijing is important for understanding the rapid evolution of haze and for developing cost-effective air pollution mitigation strategies. Here we present the first observations of the oxygen-17 excess of $PM_{2.5}$ sulfate ($\Delta^{17}O(SO_4^{2-})$) collected in Beijing haze from October 2014 to January 2015, to constrain possible sulfate formation pathways. Throughout the sampling campaign, the 12h-averaged $PM_{2.5}$ concentrations ranged from 16 to 323 μg m^{-3} with a mean of (141±88 (1σ)) μg m^{-3}, with SO_4^{2-} representing 8–25% of $PM_{2.5}$ mass. The observed $\Delta^{17}O(SO_4^{2-})$ varied from 0.1‰ to 1.6‰ with a mean of (0.9±0.3)‰.$\Delta^{17}O(SO_4^{2-})$increased with $PM_{2.5}$ levelsin October 2014 while the opposite trendswere observed in November 2014 to January 2015. Heterogeneous sulfate production rate (P_{het}) on aerosols was estimated to enhance with $PM_{2.5}$ levels, generally dominating sulfate formation during haze days when cloud liquid water content (LWC) was low. When LWC was high, however, in-cloud reactions would dominate haze sulfate formationwith a fractional contribution up to 68%. For the specific mechanisms of heterogeneous oxidation of SO_2, chemical reaction kinetics calculations suggest S(IV) (= $SO_2{\cdot}H_2O$ + HSO_3^- + SO_3^{2-}) oxidation by H_2O_2 in aerosol water accounted for 5–13% of P_{het}. The relative importance of heterogeneous sulfate production by other mechanisms was constrained by our observed $\Delta^{17}O(SO_4^{2-})$. Heterogeneous sulfate production via S(IV) oxidation by O_3 was estimated to contribute 21–22% of P_{het} on average. Heterogeneous sulfate production pathways that result in zero-$\Delta^{17}O(SO_4^{2-})$, such as S(IV) oxidation by NO_2in aerosol water and/or by O_2 on acidic microdroplets via a radical chain mechanism, contributed the remain 66–73% of P_{het}. The assumption about the thermodynamic state of aerosols

Atmos. Chem. Phys. Discuss., https://doi.org/10.5194/acp-2017-977
Manuscript under review for journal Atmos. Chem. Phys.
Discussion started: 6 November 2017
© Author(s) 2017. CC BY 4.0 License.

Atmospheric Chemistry and Physics Discussions

(stable or metastable) was found to significantly influence the calculated aerosol pH (7.6±0.1 or 4.7±1.1, respectively), and thus influence the relative importance of heterogeneous sulfate production via S(IV) oxidation by NO_2 and by O_2 on acidic microdroplets. Our calculation suggests sulfate formationvia NO_2oxidation can be the dominant pathway in aerosols at high pH-conditions calculated assuming stable state while S(IV) oxidation by O_2 on acidic microdroplets can be the dominant pathway providing that highly acidic aerosols (pH≤ 3) exist . Our results also illustrate the utility of $\Delta^{17}O(SO_4^{2-})$ for quantifying sulfate formation pathways and its inclusion in models may improve our understanding of rapid sulfate formation during haze events.

1 Introduction

Frequent occurrence of haze events in Beijing and throughout the North China Plain (NCP) during cold seasons is a health threat for round 400 million people living there. High concentrations of $PM_{2.5}$ (particulate matter with an aerodynamic diameter less than 2.5 μm), of which the daily average can exceed 300 μg m^{-3} during severe haze(He et al., 2014;Jiang et al., 2015), contribute to cardiovascular morbidity and mortality(Brook et al., 2010;Cheng et al., 2013). As one of the major components of $PM_{2.5}$, sulfate is of particular concern due to its high concentrations in haze days (Zheng et al., 2015b;Zheng et al., 2015a) and its key role in the climate system (Seinfeld and Pandis, 2012). Hourly sulfate concentrations can exceed 100 μg m^{-3} and account for up to one quarter of $PM_{2.5}$ mass during severe haze (Zheng et al., 2015a). However, due to the generally low solar radiation and cloud liquid water content (LWC) during haze (Zheng et al., 2015a;Wang et al., 2014), conventional sulfate formation via OH oxidation in the gas-phase and from aqueous-phase SO_2 (referred to as S(IV) = $SO_2{\cdot}H_2O + HSO_3^- + SO_3^{2-}$) oxidation by H_2O_2(McArdle and Hoffmann, 1983), O_3(Hoffmann and Calvert, 1985), and O_2via a radical chain mechanism initiated by transition metal ions (TMIs) in clouds (Ibusuki and Takeuchi, 1987;Alexander et al., 2009;Harris et al., 2013) cannot explain the observed high sulfate concentrations (Wang et al., 2014). To explain the observed high sulfate concentrationsduring haze in Beijing and NCP, recent studies have suggested that heterogeneous reactions on/in aerosols/aerosol water are potentially important (He et al., 2014;Hung and Hoffmann, 2015;Cheng et al., 2016;Wang et al., 2016;Zheng et al., 2015a;Zheng et al., 2015b;Wang et al., 2014). In particular, Zheng et al.(2015a) largely improved the underestimate of modelled sulfate concentrations in 2013 Beijing haze by using a relative humidity (RH)-dependent uptake coefficient (γ) of SO_2 on aerosols, without knowing the specific mechanisms of heterogeneous oxidation of SO_2. Hung and Hoffmann(2015)proposed that rapid S(IV) oxidation by O_2via a radical chain mechanism initiated due to the speciality of interfacial water on acidic microdroplets (pH ≤ 3) could be responsible for heterogeneous sulfate production in Beijing haze, while Cheng et al.(2016) suggested that S(IV) oxidation by NO_2(Lee and Schwartz, 1982;Clifton et al., 1988) in aerosol water could be important due to the high RH and NO_2 concentrations during severe haze in NCP. Due to the strong pH-dependence of these two pathways and the large variability of model calculated aerosol pH in Beijing haze (Cheng et al., 2016;Wang et al., 2016;Liu et al., 2017), the relative importance of these two pathways is difficult to constrain.

Atmos. Chem. Phys. Discuss., https://doi.org/10.5194/acp-2017-977
Manuscript under review for journal Atmos. Chem. Phys.
Discussion started: 6 November 2017
© Author(s) 2017. CC BY 4.0 License.

Atmospheric Chemistry and Physics Discussions

The oxygen-17 excess ($\Delta^{17}O$) of sulfate, defined as $\Delta^{17}O=\delta^{17}O-0.52\times\delta^{18}O$ wherein $\delta^{X}O=(({}^{X}O/{}^{16}O)_{sample}/({}^{X}O/{}^{16}O)_{VSMOW}-1)$ with X = 17 or 18 and VSMOW referring to Vienna Standard Mean Ocean Water(Matsuhisa et al., 1978), is a useful tool for estimating the relative importance of different sulfate formation pathways because each oxidant transfers its $\Delta^{17}O$ signature to the product (Table 1) through SO_2 oxidation (Savarino et al., 2000). SO_2 has $\Delta^{17}O$ = 0‰ due to the rapid isotopic exchange with abundant vapour water whose $\Delta^{17}O$ is near 0‰(Holt et al., 1981). S(IV) oxidation by H_2O_2 and O_3 leads to $\Delta^{17}O(SO_4^{2-})$ = 0.7‰ and 6.5‰, respectively, on the basis of $\Delta^{17}O(H_2O_2)$ = 1.4‰(Savarino and Thiemens, 1999)and assuming $\Delta^{17}O(O_3)$ = 26‰ (Vicars and Savarino, 2014;Ishino et al., 2017). All other sources of sulfate exhibit $\Delta^{17}O(SO_4^{2-})$ at or near 0‰. Specifically, sulfate directly emitted from natural and anthropogenic sources or formed by OH and O_2oxidation has $\Delta^{17}O(SO_4^{2-})$ values at or near 0‰ (Dubey et al., 1997;Luz and Barkan, 2005;Lee et al., 2002;Bao et al., 2000). Sulfate produced by NO_2 oxidation is suggested to occur either via a radical chain mechanism (Shen and Rochelle, 1998) or via oxygen-atom transfer from O_2(He et al., 2014), resulting in $\Delta^{17}O(SO_4^{2-})$ = 0‰. Once formed, atmospheric sulfate does not undergo further isotopic exchange, thus $\Delta^{17}O(SO_4^{2-})$ will not be altered by mass-dependent processes such as deposition.

In this work, we report the first observations of $PM_{2.5}$ $\Delta^{17}O(SO_4^{2-})$ during haze events from October 2014 to January 2015 in Beijing, and use them to quantify the relative importance of different sulfate formation pathways.

2 Materials and Methods

2.1 Sampling and atmospheric observations

A high volume air sampler (model TH-1000C II, Tianhong Instruments Co., Ltd, China) with quartz microfiber filter (Whatman Inc., UK, pre-combusted at 450°C for 4 h) was used to collect $PM_{2.5}$ samples at a flow rate of 1.05 m^3 min^{-1} from October 2014 to January 2015. The collections lasted for 12 h (08:00–20:00 LT or 20:00–08:00 LT) for each sample. The sample site is located on the rooftop of the First Teaching Building at the campus of University of the Chinese Academy of Sciences (40.41°N, 116.68°E, round20 m from the ground) in Beijing, round60 km northeast of downtown. Hourly $PM_{2.5}$, SO_2, NO_2 and O_3 concentrations were observed at Huairou station (40.33°N, 116.63°E) by Beijing Municipal Environmental Monitoring Center, which is about 10 km from our aerosol sampling site. The concentration of atmospheric H_2O_2 was not observed in our campaign, but long-term observations from March to November in Beijing shows a good correlation between H_2O_2 concentrations (ppb) and air temperature (T, in °C) according to $[H_2O_2]=0.1155\times e^{(0.0846\times T)}$(Fu, 2014). In the present study, H_2O_2 concentrations is estimated from our measured T with the above empirical equation. Our calculated H_2O_2 concentration based on this formula in October and November 2014 is respectively (0.32±0.08) ppb and (0.17±0.04) ppb, comparable to the observed values of (0.44±0.18) ppb and (0.38±0.11) ppb, respectively in October and November 2013 (Fu, 2014). Meteorological data including T and relative humidity (RH) were recorded by an automatic weather station (model MetPak with integrated wind sonic, Gill Instruments Limited, UK). Time reported in this paper is local time (LT = UTC + 8).

Atmos. Chem. Phys. Discuss., https://doi.org/10.5194/acp-2017-977
Manuscript under review for journal Atmos. Chem. Phys.
Discussion started: 6 November 2017
© Author(s) 2017. CC BY 4.0 License.

Atmospheric Chemistry and Physics Discussions

2.2 Measurements of ions and isotope ratios

A detailed description of the method for chemical analysis of NH_4^+, K^+, Ca^{2+}, Na^+, Mg^{2+}, SO_4^{2-}, NO_3^- andCl^- can be found in the literature (Ye et al., 2015). Briefly, ions were extracted from a part (2 cm × 2 cm) of each filter with 20 ml of Millipore water (≥ 18 MΩ) by sonication for 80 min in an ice water bath. Insoluble substances in the extract were filtered with 0.45 μm filters before analysis. Then the pH of filtrates was measured by an ion activity meter (model PXS-215, Shanghai INESA Scientific Instrument Co., Ltd., China). And the ion concentrations were analysed using Dionex ICS-2100 ion chromatograph system (Thermo Fisher Scientific Inc., USA). The preparation and measurements of $\Delta^{17}O(SO_4^{2-})$ were conducted in Isolab at the University of Washington, USA. A detailed description of the method can be found in the literature (Savarino et al., 2001;Geng et al., 2013). Briefly, $PM_{2.5}$ sample filters were dissolved in Millipore water (≥ 18 MΩ) and the insoluble substances were filtered. Pre-packed ion capture cartridges (Alltech Maxi-Clean IC-RP SPE) were used for the first step of removal of organics. Cations in the samples were replaced with sodium using a cation exchange resin and 30% H_2O_2 solution was added as the second step of removal of organics. Excess H_2O_2 was removed via evaporation and SO_4^{2-} was separated from other ions in solution by ion chromatography. After ion separation, SO_4^{2-} was converted to Ag_2SO_4, dried, and then pyrolyzed at 1000°C in an elemental analyzer to form Ag(s), SO_2(g), and O_2(g). The produced gases were carried by He gas to pass through a liquid nitrogen trap to remove SO_2, and then a GC to further purify the O_2 gas which was finally induced to a mass spectrometer (Thermo Scientific MAT 253). Masses of 32, 33 and 34 of O_2 were measured to determine $\delta^{17}O$ and $\delta^{18}O$ and then $\Delta^{17}O$ was calculated. The precision of $\Delta^{17}O$ measurement in this method is ±0.3‰ based on replicate analysis of standards. To quantify the uncertainty in each sample, 30 samples were measured in triplicate, 2 samples in quadruplicate, and 2 samples in duplicate depending on the limitation of sample size. Totally, 10 filters sampled in non-polluted days (NPD, $PM_{2.5}$< 75 μg m^{-3}) and 24 filters sampled in polluted days (PD, $PM_{2.5}$≥ 75 μg m^{-3}) were analysed.

2.3 Estimate of the overall rate of heterogeneous sulfate production

Heterogeneous sulfate production (P_{het}) is commonly parameterized in models according to Eq. (1) (Jacob, 2000;Zheng et al., 2015a):

$$P_{het} = \frac{3600\times96}{RT}\left(\frac{R_p}{D_g}+\frac{4}{v\gamma}\right)^{-1} S_p[SO_2(g)] \quad (1)$$

where P_{het} is in unit of μg m^{-3} h^{-1}, 3600 is a time conversion factor (s h^{-1}), 96 is the molar mass of SO_4^{2-} (g mol^{-1}), R is the gas constant (0.082 atm L K^{-1} mol^{-1}), and T is temperature in K. R_p is the radius of aerosol particles (m), D_g is the gas-phase molecular diffusion coefficient of SO_2 (m^2 s^{-1}), v is the mean molecular speed of SO_2 (g) (m s^{-1}), $\gamma$is the uptake coefficient of SO_2 on aerosols (unitless), [SO_2 (g)] is the gas-phase concentration of SO_2 (ppb) and S_p is the aerosol surface area per unit volume of air (m^2 m^{-3}). The typical tropospheric value of D_g and v is 2×10^{-5} m^2 s^{-1} and 300 m s^{-1}, respectively (Jacob, 2000). Observations of $PM_{2.5}$ mass concentrations (μg m^{-3}) and $PM_{2.5}$ mean radius (m) during Beijing haze roughly follows an empirical formula: $R_p = (0.254\times PM_{2.5}+10.259)\times10^{-9}$ (Guo et al., 2014). By using the volume and surface area formulas of a sphere and the mean density of particles (ρ= 1.5×10^6 g m^{-3}(Guo et al., 2014)), S_p can be estimated from Eq. (2). A RH-

Atmos. Chem. Phys. Discuss., https://doi.org/10.5194/acp-2017-977
Manuscript under review for journal Atmos. Chem. Phys.
Discussion started: 6 November 2017
© Author(s) 2017. CC BY 4.0 License.

Atmospheric Chemistry and Physics Discussions

dependent γ (= (2–5)×10^{-5}, Eq. (3)) derived from Zheng et al.(2015a)during 2013 Beijing haze was used. This range of γ is also consistent with the estimated values of γ from (1.6±0.7) to (4.5±1.1) ×10^{-5} by Wang et al.(2016).

$$S_{\mathrm{p}} = \frac{\mathrm{PM}_{2.5}\times 10^{-6}}{4/3\times\pi {R_{\mathrm{p}}}^3\times\rho} \times 4\pi {R_{\mathrm{p}}}^2 \quad (2)$$

$$\gamma = \begin{cases} 2\times 10^{-5}, \mathrm{RH} \le 50\ \% \\ 2\times 10^{-5} + \frac{5\times10^{-5}-2\times10^{-5}}{100-50}\times(\mathrm{RH}-50), \ 50\ \% \le \mathrm{RH} \le 100\ \% \end{cases} \quad (3)$$

2.4 Estimate of primary sulfate

The primary sulfate, which is directly emitted into air, includes the sea salt source, terrigenous source and anthropogenic source (Li et al., 2013;Faloona, 2009). The concentration of sea salt sulfate was calculated by using the observed concentrations of SO_4^{2-} and Na^+ and the mass ratio of (SO_4^{2-}/Na^+) = 0.252 in seawater (Calhoun et al., 1991). The terrigenous sulfate was estimated using the observed concentrations of SO_4^{2-} and Ca^{2+} and the mass ratio of (SO_4^{2-}/Ca^{2+}) = 0.18 in soil (Legrand et al., 1997), where (Ca^{2+}/Na^+) = 0.038 in seawater was used to calculate the fraction of observed Ca^{2+} from soil (Legrand and Mayewski, 1997). The anthropogenic primary sulfate is estimated as 3% of anthropogenic SO_2 emissions in models (Faloona, 2009;Alexander et al., 2009). Supposing all the observed concentrations of SO_2 and precursors of secondary sulfate are anthropogenic, we have n_{ap} = 3% × (n_{SO2} + n_{sas}), where n_{sas} = n_{tos}–n_{ss}–n_{ts}–n_{ap} and n_{ap}, n_{sas}, n_{tos}, n_{ss} and n_{ts} is the molar concentrations of anthropogenic primary sulfate (ap), secondary sulfate (sas), total sulfate (tos), sea salt sulfate (ss) and terrigenous sulfate (ts). The estimated concentration of total primary sulfate is the sum of primary sulfate from all these sources.

2.5 Estimate of sulfate production rate from OH oxidation in the gas-phase

The sulfate production rate from OH oxidation in the gas-phase (P_{SO2+OH}) can be expressed as:

$$P_{\mathrm{SO_2+OH}} = \frac{3600\times 96\times R_{\mathrm{SO_2+OH}}}{RT} \quad (4)$$

whereP_{SO2+OH} is in unit of μg m^{-3} h^{-1}, 3600, 96, R and T is the same as Eq. (1).R_{SO2+OH} is the chemical reaction rate (ppb s^{-1}), calculated as shown in Table S1 and S2.

2.6 Estimate of in-cloud sulfate production rate

The main in-cloud sulfateformation pathways considered here include S(IV) oxidation by H_2O_2, O_3, NO_2(Wang et al., 2016) and O_2 via a radical chain mechanism initiated by TMIs(Alexander et al., 2009). Their chemical reaction rate expressions ($R_{S(IV)+oxi}$) and rate constants (k) are summarized in Table S3. The rate of in-cloud sulfate production by a certain oxidant ($P_{cloud,\ S(IV)+oxi}$) can be expressed as(Seinfeld and Pandis, 2012):

$$P_{\mathrm{cloud},S(\mathrm{IV})+\mathrm{oxi}} = 3600\times 96\times \mathrm{LWC}\times R_{S(\mathrm{IV})+\mathrm{oxi}} \quad (5)$$

© Author(s) 2017. CC BY 4.0 License.

Where $P_{cloud,\ S(IV)+oxi}$ is in unit of μg m^{-3} h^{-1}, 3600 and 96 is the same as Eq. (1), and $R_{S(IV)+oxi}$ is in unit of M s^{-1}. Cloud liquid water content (LWC, in unit of mg m^{-3}) was derived from a global reanalysis, GEOS-FP (https://gmao.gsfc.nasa.gov/products/).

2.7 Isotopic constrainson sulfateformation pathways

Since S(IV) oxidation by O_3 and H_2O_2 are the sole sources of non-zero $\Delta^{17}O(SO_4^{2-})$(Table 1), the relative importance of different sulfate formation pathways can be calculated as follows (Alexander et al., 2012):

$$\Delta^{17}O_{obs} = \left(6.5 \times f_{S(IV)+O_3}\right) + \left(0.7 \times f_{S(IV)+H_2O_2}\right) + \left(0 \times f_{zero-\Delta^{17}O}\right) \quad (6)$$

where $f_{S(IV)+O3}$ and $f_{S(IV)+H2O2}$ are the fractional contributions of S(IV) oxidation by O_3 and H_2O_2 oxidation to total sulfate production, respectively, and $f_{zero-\Delta17O}$ represents the fractional contribution of sulfate with zero-$\Delta^{17}O$ processes such as primary sulfate, secondary sulfate formed via OH oxidation, NO_2 oxidation, and O_2 oxidation via a radical chain reaction initiated by TMIs in cloudsor due to the speciality of interfacial water on acidic microdroplets. By definition, we have $f_{S(IV)+O3} + f_{S(IV)+H2O2} + f_{zero-\Delta17O} = 100\%$.

In addition, as sulfate with non-zero $\Delta^{17}O(SO_4^{2-})$ is produced either via in-cloud reactions or via heterogeneous reactions or both, Eq. (6) can also be written as follows:

$$\Delta^{17}O_{obs} = f_{het} \times \Delta^{17}O_{het} + f_{cloud} \times \Delta^{17}O_{cloud} + f_{SO_2+OH} \times \Delta^{17}O_{SO_2+OH} + f_p \times \Delta^{17}O_p \quad (7)$$

Where f_{het}, f_{cloud}, f_{SO2+OH} and $f_p$respectivelyrepresents the fractional contribution of heterogeneous sulfate production, in-cloud sulfate production, gas-phase sulfate production and primary sulfate to the observed sulfate.$\Delta^{17}O_{het}$, $\Delta^{17}O_{cloud}$, $\Delta^{17}O_{SO2+OH}$ and $\Delta^{17}O_p$ respectively represents $\Delta^{17}O$ of corresponding sulfate produced via above pathways. Both $\Delta^{17}O_{SO2+OH}$ and $\Delta^{17}O_p$ is equal to 0‰. $\Delta^{17}O_{cloud}$ can be calculated as Eq. (8) due to thatlifetime of sulfate produced in clouds will not depend on the specific S(IV) oxidant.

$$\Delta^{17}O_{cloud} = \frac{6.5 \times P_{cloud,\ S(IV)+O_3} + 0.7 \times P_{cloud,\ S(IV)+H_2O_2}}{P_{cloud}} \quad (8)$$

Where P_{cloud} is the rate of total in-cloud sulfate production, which was calculated as the sum of in-cloud S(IV) oxidation by H_2O_2, O_3, NO_2 and O_2initiated by TMIs.

2.8 The prediction of aerosol water content (AWC), aerosol pH and ionic strength (I_s)

AWC, aerosol pHand I_s was calculated by the ISORROPIA II model, which is a thermodynamic equilibrium model for NH_4^+-K^+-Ca^{2+}-Na^+-Mg^{2+}-SO_4^{2-}-NO_3^--Cl^--H_2O aerosols (Fountoukis and Nenes, 2007). The ISORROPIA II model can solve forward problems in which *T*, RH and the concentrations of gas + aerosols are known (eg: NH_3 + NH_4^+), and reverse problems in which *T*, RH and the concentrations of aerosol (but not gas) species are known. We used the forward method to calculate AWC, aerosol pH and I_s as this method has been shown to best predict aerosol pH (Hennigan et al., 2015). The AWC, pH and I_s was firstly calculated in metastable mode (assuming that bulk aerosol solution is supersaturated), which is consistent with previous studiesabout Beijing haze (Liu et al., 2017;Guo et al., 2017). However, the work ofRood et al.(1989)

Atmos. Chem. Phys. Discuss., https://doi.org/10.5194/acp-2017-977
Manuscript under review for journal Atmos. Chem. Phys.
Discussion started: 6 November 2017
© Author(s) 2017. CC BY 4.0 License.

Atmospheric Chemistry and Physics Discussions

in California, USA suggested that not all aerosolsare in metastable state, even though the fractional occurrence of metastable aerosolsincreases with increasing RH in urban sites (i.e., from near 0 at RH <round 30% to near 100 % at RH > round 80%, roughly following Eq. (9)). So we also predicted the AWC, pH and I_s in stable mode (assuming that bulk aerosols crystallize once saturation is exceeded), which is consistent with Wang et al.(2016).The input of observed inorganic ion concentrations and meteorological parametersare summarized in Table S4. Since gaseous NH_3 was not measured in our campaign, we used the empirical equation NH_3 (ppb) = 0.34×NO_X(ppb)+0.63, derived from observations of Meng et al.(2011) in Beijing winter, to estimate the NH_3 concentrations. We used NO_2 concentrations instead of NO_X as input due to the lack of NO_X observations in our study, which would give a lower end of the NH_3 concentrations. Given the importance of AWC for reaction rates and the fact that ISORROPIA II underestimates AWC at low RH (Bian et al., 2014), samples with RH < 40% are excluded from analysis (Hennigan et al., 2015). This excludes 8 out of the total 34 samples (24%), with 6 of them in NPD. A total of 4 samples in NPD and 22 samples in PD were analysed for AWC, aerosol pH and I_s using observations and the ISORROPIA II model. Due to that the predicted I_s is high (I_s> 10 M, Table S4), which suggests aerosol water is non-ideal, the influence of I_s on reaction rate constants (Table S3) and effective Henry's law constants (Table S5) is taken into considerationwhen the influence is known.

$$\mathrm{MF} = \begin{cases} 0, & \mathrm{RH} < 30\ \% \\ -0.024 \times \mathrm{RH}^2 + 4.18 \times \mathrm{RH} - 89.13, & 30\ \% \le \mathrm{RH} \le 80\ \% \\ 100\ \%, & 80\ \% < RH \le 100\ \% \end{cases} \quad (9)$$

where MF (in %) is the fraction of metastable aerosols to total aerosols.

2.9 Estimate of aqueous concentrations of trace species

The aqueous concentrations of SO_2, O_3, H_2O_2 and NO_2 were calculated as described in Table S5. The determination of in-cloud concentrations of TMIs (here only Fe(III) and Mn(II) (Alexander et al., 2009)) is described below.

The concentration of soluble Fe(III) follows Eqs. (10)–(13)(Liu and Millero, 1999):

$$\log_{10}[\mathrm{Fe(III)}] = \log_{10} K^*_{\mathrm{Fe(OH)_3}} + 3 \times \log_{10}[\mathrm{H^+}] + \log_{10}(1 + \beta_1^*[\mathrm{H^+}]^{-1} + \beta_2^*[\mathrm{H^+}]^{-2}) \quad (10)$$

where

$$\log_{10} K^*_{\mathrm{Fe(OH)_3}} = -13.486 - 0.1856 \times I_s^{0.5} + 0.3073 \times I_s + 5254/T \quad (11)$$

$$\log_{10} \beta_1^* = 2.517 - 0.8885 \times I_s^{0.5} + 0.2139 \times I_s - 1320/T \quad (12)$$

$$\log_{10} \beta_2^* = 0.4511 - 0.3305 \times I_s^{0.5} - 1996/T \quad (13)$$

and [Fe(III)] is the aqueous concentration of Fe(III) in unit of M, T is temperature in unit of K, and I_s is ionic strength in unit of M, $K^*_{\mathrm{Fe(OH)3}}$ is the solubility product constant of $Fe(OH)_3$, and β^*_1 and β^*_2 is respectively first-order and second-order cumulative hydrolysis constants of Fe^{3+}.

Our calculation suggests in-cloud [Fe(III)] was in the range of 0.6 to 6.1 μM with a mean of (2.6±1.8) μM, which is similar to the observed values in NCP(Guo et al., 2012;Shen et al., 2012). The concentration of soluble Mn(II) in cloud water

© Author(s) 2017. CC BY 4.0 License.

was set to be 1 μM in the present study, which is the general value observed in cloud water in NCP (Guo et al., 2012;Shen et al., 2012).

2.10 Estimate of sulfate production rate in aerosol water

The reaction rate expressions, rate constants (k) and the influence of I_s on k for sulfate production in aerosol water are summarized in Table S3. The overall rates for S(IV) oxidation in aerosol water depend not only on chemical reaction rates (Table S3) but also on the mass transport limitations. A standard resistance model was used to estimate effects of mass transport following the work ofCheng et al.(2016):

$$\frac{1}{R_{\mathrm{H,S(IV)+oxi}}} = \frac{1}{R_{\mathrm{S(IV)+oxi}}} + \frac{1}{J_{\mathrm{aq,lim}}} \quad (14)$$

where $R_{\mathrm{H,\ S(IV)+oxi}}$ is the overall reaction rate for S(IV) oxidation by a certain oxidant (oxi) such as O_3, H_2O_2, NO_2 and O_2on acidic microdroplets (M s^{-1}), $R_{\mathrm{S(IV)+oxi}}$ is the chemical reaction rate (M s^{-1}) and $J_{\mathrm{aq,\ lim}}$ is the rate limited by mass transfer from the gas to the aqueous phase (M s^{-1}). $R_{\mathrm{S(IV)+oxi}}$ was calculated as described in Table S3. The limiting mass transfer $J_{\mathrm{aq,\ lim}}$ was calculated by Eqs.(15) and (16).

$$J_{\mathrm{aq,lim}} = \min\left\{J_{\mathrm{aq}}(\mathrm{SO_2}), J_{\mathrm{aq}}(\mathrm{oxi})\right\} \quad (15)$$

$$J_{\mathrm{aq}}(\mathrm{X}) = k_{\mathrm{MT}}(\mathrm{X}) \times [\mathrm{X(aq)}] \quad (16)$$

where X = SO_2, O_3, H_2O_2 or NO_2 and k_{MT} (s^{-1}) is the mass transfer rate coefficient and was calculated as Eq. (17)(Cheng et al., 2016;Seinfeld and Pandis, 2012):

$$k_{\mathrm{MT}}(\mathrm{X}) = \left[\frac{R_{\mathrm{p}}^2}{3D_{\mathrm{g}}} + \frac{4R_{\mathrm{p}}}{3\alpha v}\right]^{-1} \quad (17)$$

Where R_p, D_g and v are the same as Eq.(1). The α used in our calculation is respectively 0.11 for SO_2, 0.23 for H_2O_2, 2.0×10^{-3} for O_3 and 2.0×10^{-4} for NO_2(Seinfeld and Pandis, 2012;Jacob, 2000). The term on the left hand side of Eq.(17) is the gas-phase diffusion limitation while the term on the right hand side of Eq. (17) is the interfacial mass transport limitation. k_{MT} was limited by interfacial mass transport limitation in our study.

The rate of heterogeneous sulfate production by a certain oxidant ($P_{\mathrm{het,\ S(IV)+oxi}}$) in aerosol water can be expressed as:

$$P_{\mathrm{het,S(IV)+oxi}} = 3600 \times 96 \times \mathrm{AWC} \times R_{\mathrm{H,S(IV)+oxi}} \quad (18)$$

Where $P_{\mathrm{het,\ S(IV)+oxi}}$ is in the unit of μg m^{-3} h^{-1}, 3600 and 96 is the same as Eq. (1). AWC is in the unit of mg m^{-3} and $R_{\mathrm{H,\ S(IV)+oxi}}$ is in the unit of M s^{-1}, For $R_{\mathrm{H,\ S(IV)+oxi}}$, our calculation suggested that the role of mass transport limitationsfor S(IV) oxidation by NO_2 was significant at high pH values.

Atmos. Chem. Phys. Discuss., https://doi.org/10.5194/acp-2017-977
Manuscript under review for journal Atmos. Chem. Phys.
Discussion started: 6 November 2017
© Author(s) 2017. CC BY 4.0 License.

Atmospheric Chemistry and Physics Discussions

3 Results and Discussion

3.1 Characteristics of haze events in Beijing

Figure 1ashows the temporal evolution of concentrations of $PM_{2.5}$ and SO_4^{2-} during our sampling period. The 12h-averaged $PM_{2.5}$ concentrations ranged from 16 to 323 μg m^{-3} with a mean of (141±88 (1σ)) μg m^{-3}. In comparison, the Grade II of the Chinese National Ambient Air Quality Standard of daily $PM_{2.5}$ is 75 μg m^{-3}. The SO_4^{2-} concentrations varied from 1.5 to 56.4 μg m^{-3} with a mean of (21.2±15.4) μg m^{-3}. As shown in Fig. 1a, SO_4^{2-} concentrations presented a similar temporal trend as $PM_{2.5}$ concentrations, i.e., increased from a mean of (3.9±1.8) μg m^{-3} in non-polluted days (NPD, $PM_{2.5}$< 75 μg m^{-3}) to (28.4±12.5) μg m^{-3} in polluted days (PD, $PM_{2.5}\geq$ 75 μg m^{-3}). The fraction of $SO_4^{2-}$to $PM_{2.5}$ mass concentration ranged from 8–25%, and increased from a mean of (11±2)% in NPD to (15±5)% in PD. The sulfur oxidation ratio (SOR = $nSO_4^{2-}/(nSO_4^{2-}+nSO_2)$, where nSO_4^{2-} and nSO_2 represents the molar concentration of SO_4^{2-} and SO_2, respectively), a proxy for secondary sulfate formation (Sun et al., 2006), also increased rapidly with $PM_{2.5}$ levels, from a mean of (0.12±0.04) in NPD to (0.41±0.17) in PD (Fig. 1b).

Observed $\Delta^{17}O(SO_4^{2-})$ ($\Delta^{17}O_{obs}$) ranged from 0.1‰ to 1.6‰ with a mean of (0.9±0.3)‰ (Fig. 1b). The highest $\Delta^{17}O_{obs}$ = 1.6‰ occurred during PD of Case II in October 2014 while the lowest $\Delta^{17}O_{obs}$ = 0.1‰ occurred during PD of Case IV in December 2014. $\Delta^{17}O_{obs}$ reported here is similar in magnitude to previous observations of $\Delta^{17}O(SO_4^{2-})$ in aerosols and rainwater collected at other mid-latitude sites (Table S6). The overall $\Delta^{17}O_{obs}$ levels during our entire sampling time are similar for NPD and PD, being (0.9±0.1)‰ and (0.9±0.4)‰, respectively. However, the NPD to PD difference of $\Delta^{17}O_{obs}$ can be case-dependent. For Case I and II in October 2014, $\Delta^{17}O_{obs}$ increased from NPD to PD, while the opposite trend is observed for Case III to V in November 2014 to January 2015 (Fig. 2a). These $\Delta^{17}O_{obs}$ variations are generally similar to variability in concentrations of observed O_3 and calculated H_2O_2(Fig. 2b&c), which is consistent with the fact that O_3 and H_2O_2 are the sole sources of non-zero $\Delta^{17}O(SO_4^{2-})$ (Table 1).

3.2 Direct estimate of sulfate formation pathways based on $\Delta^{17}O_{obs}$

The fact that $\Delta^{17}O_{obs}$ falls out of the range of any single reaction pathway suggests that sulfate in Beijing haze must be produced by multiple reactions. Figure3 shows the calculated possible fractional contributions of each formation pathway ($f_{S(IV)+H2O2}$, $f_{S(IV)+O3}$, and $f_{zero\text{-}\Delta17O}$) for each sample using Eq. (6). On average over all samples collected, $f_{S(IV)+O3}$ = 4–13%, $f_{S(IV)+H2O2}$ = 0–88%, and $f_{zero\text{-}\Delta17O}$ = 8–87%. For samples during PD of Case IV in December 2014 with the three lowest $\Delta^{17}O_{obs}$ values (Fig. 1b), $f_{zero\text{-}\Delta17O}$ was respectively in the range of 57–95%, 86–98% and 57–95%, corresponding to $f_{S(IV)+H2O2}$ being in the range of 0–43 %, 0–14 % and 0–43% respectively, which suggests zero-$\Delta^{17}O$ pathways clearly dominated sulfate formation during PD of Case IV. However, for other samples, the maximum possible $f_{S(IV)+H2O2}$ ranged from 71 to 100% with a mean of (93±7)% while the maximum possible $f_{zero\text{-}\Delta17O}$ was 75 to 92% with a mean of (86±4)%, implying that sulfate formation during these sampling periods were dominated by H_2O_2 oxidation and/or zero-$\Delta^{17}O$ pathways.

Atmos. Chem. Phys. Discuss., https://doi.org/10.5194/acp-2017-977
Manuscript under review for journal Atmos. Chem. Phys.
Discussion started: 6 November 2017
© Author(s) 2017. CC BY 4.0 License.

Atmospheric Chemistry and Physics Discussions

3.3 Chemical kinetic calculations with the constraint of $\Delta^{17}O_{obs}$

The good correlation between RH and SOR in Fig. 4a ($r = 0.76$, $p < 0.01$) suggests heterogeneous reactions played an important role in sulfate formation. Our calculations show that overall heterogeneous sulfate production (P_{het}, see Sect. 2.3) presented similar trends with $PM_{2.5}$ concentrations (Fig. 4b) and increased from a mean of (0.6±0.3) μg m^{-3} h^{-1} in NPD to (2.0±1.1) μg m^{-3} h^{-1} in PD during our sampling period. In comparison, Cheng et al.(2016) reported that the missing sulfate production rate required to explain the observed sulfate concentration is around 0.07 μg m^{-3} h^{-1} when $PM_{2.5}$< 50 μg m^{-3} and around 4 μg m^{-3} h^{-1} when $PM_{2.5}$> 400 μg m^{-3} during 2013 Beijing haze. We also calculate the contribution from primary sulfate and perform chemical kinetic calculations including SO_2 oxidation by OH in the gas-phase and in-cloud sulfate production (Fig. 5, see Sect. 2.4–2.6)to estimate the relative importance of heterogeneous sulfate production during haze in our sampling period. Heterogeneous reactions were found to dominate sulfate formation during PD in four out of the total five Cases with fractional contribution of 42 to 54% and a mean of (48±5)% (Fig. 5). This is consistent with Zheng et al.(2015a) who reported that about half of the observed sulfate was from heterogeneous reactionsduring 2013 Beijing haze. In contrast, we found that during PD of Case II in October 2014, heterogeneous sulfate production only accounted for 23% of total sulfate production while in-cloud sulfate production predominated total sulfate production with an estimated fraction of 68%. The predominant role of in-cloud sulfate production in PD of Case II was supported by the relative high LWC during this time period (Fig. 6a). Our calculations also suggest the in-cloud sulfate production was dominated by H_2O_2 oxidation throughout our sampling period (Fig. 6b), which is consistent with previous findings that H_2O_2 oxidation is the most important in-cloud sulfate production pathway globally (Seinfeld and Pandis, 2012) and in NCP (Shen et al., 2012). In addition, the $\Delta^{17}O$ of sulfate produced in clouds ($\Delta^{17}O_{cloud}$) was estimated to range from 0.5‰ to 0.8‰ with a mean of (0.6±0.1)‰ during our sampling period and showed similar variations with $\Delta^{17}O_{obs}$(Fig. 6c). The mean value of $\Delta^{17}O_{cloud}$calculated here is close to $\Delta^{17}O(SO_4^{2-})$ in rainwater observed in central China (0.53±0.19 ‰) (Li et al., 2013) and at Baton Rouge, USA (0.62±0.32 ‰) (Jenkins and Bao, 2006).In addition, by using Eq. (7), the$\Delta^{17}O$ of sulfate produced via heterogeneous reactions($\Delta^{17}O_{het}$) was calculated to range from 0.1 ‰ to 3.1‰ in our study.

To explore the specific mechanisms of heterogeneous oxidation of SO_2, we calculate aerosol parameters such as aerosol water content (AWC), pH and ionic strength (I_s) by using the ISORROPIA II thermodynamic model (Fountoukis and Nenes, 2007)(Fig.7, see Sect. 2.8). It was found that the assumptions about aerosol thermodynamic state (salts crystallize once saturation is exceeded, termed as “stable state” or aerosol solution is supersaturated, termed as “metastable state”) significantly influence the calculated aerosol pH, but have little impact on the calculated AWC and I_s(Fig. 7). Calculated AWC increased with $PM_{2.5}$ concentrations, from (5.3±7.4) μg m^{-3} in NPD to (63.5±54.6) μg m^{-3} in PD when assuming stable state and from (9.6±6.0) μg m^{-3} in NPD to (84.2±49.2) μg m^{-3} in PD when assuming metastable state (Fig. 7a). Calculated I_s was similar for stable and metastable assumptions, ranging from 11.3 to 51.6 M (Fig. 7b). The high I_s suggested aerosol water was non-ideal and thus the influence of I_s on reaction rate constants (Table S3) and effective Henry’s law constants (Table S5) was taken into consideration when the influence is known. The bulk aerosol pH predicted in stable state was in

© Author(s) 2017. CC BY 4.0 License.

the range of 7.5 to 7.8 with a mean of (7.6±0.1), consistent with bulk aerosol pH (7.63±0.03) calculations during a haze event in Beijing 2015 predicted by Wang et al.(2016). The bulk aerosol pH calculated assuming metastable state was in the range of 3.4 to 7.6 with a mean of (4.7±1.1), consistent with the mean value of 4.2 calculated in metastable aerosol assumption during severe haze in Beijing 2015–2016 by Liu et al.(2017). The calculated aerosol pH assuming metastable state decreased with increasing $PM_{2.5}$ levels, from a mean of (6.5±1.3) in NPD to (4.4±0.6) in PD, while that assuming stable state shows no relationship with $PM_{2.5}$ concentrations (Fig. 7c). Our measured pH of filtrate ranged from 4.6 to 8.2 with an mean of (5.7±1.0), similar to pH of filtrate from $PM_{2.5}$ in Beijing reported by Wang et al.(2005). The measured pH of filtrate shows similar trends with bulk aerosol pH calculated assuming metastable state (Fig. 7c), with a mean value (6.9±0.7) in NPD and (5.1±0.6) in PD, which suggests that bulk aerosols are in metastable statewith moderate acidityin PD. This is also consistent with our estimate that most aerosols are in metastable with a fraction of (74±17) % in PD by using Eq. (9) and our cognition that the mixture of major acidic aerosols with minor neutralaerosols would lead to the bulk being acidic. However, as the effective Henry's law constant of SO_2 at pH= 7.6(stable state) can be 3 orders magnitude higher than that at pH = 4.4 (metastable state in PD) (Seinfeld and Pandis, 2012), the high pH could render stable state aerosols, which are minorities although, being potentiallysignificant active sites for heterogeneous sulfate production during PD.

The main heterogeneous sulfate formation pathways include S(IV) oxidation by H_2O_2, O_3, NO_2 and O_2initiated due to the speciality of interfacial water on acidic microdroplets as proposed by Hung and Hoffmann(2015). Other sulfate formation pathways such as S(IV) oxidation by NO_3 radical, methyl-hydrogenperoxide (MHP), peroxyacetic acid (PAA), and hypohalous acids in aerosol water (Feingold et al., 2002;Walcek and Taylor, 1986;Chen et al., 2017) is thought to be negligible during haze in NCP (Cheng et al., 2016), and thus is not considered here. We estimate the relative importance of main heterogeneous sulfate formation pathways as the following procedure. Firstly, the heterogeneous sulfate production rate via S(IV) oxidation by H_2O_2 ($P_{het,\ S(IV)+H2O2}$) was calculated with the influence of I_s being considered, which has been determined at high $I_s$in laboratories. Then its fractional contribution ($f_{het,\ S(IV)+H2O2}$) to overall heterogeneous sulfate production (P_{het}) calculated using apparent γ (see Sect. 2.3) was estimated. However, large uncertainties exist in the influence of I_s on the reaction rate constant of S(IV) oxidation by O_3 in aerosol water (Table S3), which prevents the estimate of its fractional contribution ($f_{het,\ S(IV)+O3}$) to P_{het} from purely chemical kinetic calculations. Instead, $f_{het,\ S(IV)+O3}$was estimated using our calculated $f_{het,\ S(IV)+H2O2}$ and $\Delta^{17}O_{het}$values, on the basis that $\Delta^{17}O(SO_4^{2-}) > 0‰$ originates solely from H_2O_2 and O_3 oxidation.Then zero-$\Delta^{17}O$ pathways such as S(IV) oxidation by NO_2in aerosol water and by O_2on acidic microdropletswas estimated to bethe remaining part ($f_{het,\ zero\text{-}\Delta17O}$). At last, the potential importance of S(IV) oxidation by NO_2 in aerosol water and O_2 on acidic microdroplets was discussed.

Calculations show that $f_{het,\ S(IV)+H2O2}$ was 4–6% with a mean of (5±1)% under stable aerosol assumptions, and 8–19% with a mean of (13±4)% under metastable state assumptions for PD of all the Cases. $f_{het,\ S(IV)+O3}$was calculated to be 2–47% with a mean of (22±17)% in stable state assumption and 0–47% with a mean of (21±18)% in metastable state assumption. Correspondingly, $f_{het,\ zero\text{-}\Delta17O}$was the remaining 73 % (47–94%) in stable assumption, or 66% (42–81%) in metastable assumption for PD of all the Cases (Fig. 8). Excluding PD of Case II, in which sulfate formation was predominated by in-

© Author(s) 2017. CC BY 4.0 License.

cloud reactions, our calculations suggest zero-$\Delta^{17}O$ pathways such as S(IV) oxidation by NO_2 in aerosol water and by O_2 on acidic microdroplets are important for sulfate formation during Beijing haze.

Cheng et al. (2016) suggested that S(IV) oxidation by NO_2 in aerosol water could largely account for the missing sulfate source in 2013 Beijing haze. In their study, the calculated mean aerosol pH is 5.8, while influence of $I_s$was not taken into account due to the lack of relevant experimental data. The calculated $P_{het, S(IV)+NO2}$ is highly sensitive to aerosol pH. In our study, when aerosol pH decreased from (7.6±0.1) assuming stable state to (4.7±1.1) assuming metastable state, mean $P_{het, S(IV)+NO2}$ decreased from (6.5±7.7) μg m^{-3} h^{-1} to (0.01±0.02) μg m^{-3} h^{-1} for PD of all the Cases (Fig. 8). The former is much larger than our estimate of overall heterogeneous production rate, P_{het} = (2.0±1.1) μg m^{-3} h^{-1}, while the latter is too small. Moreover, the influence of I_s was not considered, which, in principal, tends to increase the reaction rate constant of S(IV) oxidation by NO_2(Cheng et al., 2016). The treatment of aerosols as a bulk quantity, assuming that all aerosols are either in stable or metastable state, may lead to errors in calculating heterogeneous sulfate production rates. As stated in Sect. 2.8, not all aerosols are in metastable state, even though the fractional occurrence of metastable aerosols increases with increasing RH (Rood et al., 1989). It shows in Fig. 9athat the fraction of metastable aerosols to total aerosols (MF in %), estimated by using Eq. (9), increases with $PM_{2.5}$ levels.However, $P_{het, S(IV)+NO2}$assuming a combination of metastable and stable state as $P_{het, S(IV)+NO2}$ = MF×$P_{het, S(IV)+NO2, metastable}$ + (100 %–MF)×$P_{het, S(IV)+NO2, stable}$ can still increase with $PM_{2.5}$ levels and reach (0.9±0.7) during PD of all the Cases (Fig. 9b), much higher than $P_{het, S(IV)+NO2}$ = (0.01±0.02) μg m^{-3} h^{-1} under sole metastable aerosol assumption. This estimate suggested that even though the majority of aerosols may be in metastable state during PD (74 ± 17 % in our calculation), the high pH of the minority of aerosols in stable state could render S(IV) oxidation by NO_2 a potentially significant pathway for heterogeneous sulfate production.

Since $P_{het, S(IV)+NO2}$ using calculated aerosol pH assuming metastable state was two orders of magnitude lower than P_{het} during PD, we further examined S(IV) oxidation by O_2 on acidic microdroplets under the metastable state assumption. A laboratory study suggested that SO_2 oxidation by O_2 on acidic microdroplets has a large aqueous-phase reaction rate constant of 1.5×10^6[S(IV)] (M s^{-1}) at pH ≤ 3, a pH range much lower than our calculated pH values. The rate constant was shown to decrease with increasing pH, however, no values of the rate constant at pH > 3 was reported (Hung and Hoffmann, 2015). Fig.8b shows heterogensous sulfate production rate via S(IV) oxidation by O_2 on acidic microdroplets($P_{het, S(IV)+O2}$) with AWC calculated assuming metastable state and the aqueous-phase rate constant for pH≤ 3 being used. The estimated $P_{het, S(IV)+O2}$ was 1520.5 to 130359.1 μg m^{-3} h^{-1} with a mean of (25166.8±27266.3) μg m^{-3} h^{-1} during PD of all Cases, which is four order of magnitude larger than P_{het}. This value should be an overestimate due to our calculated bulk aerosol pH predicted in metastable state being (4.4±0.6) during PD. However, some fraction of aerosols could have pH≤ 3 due to the Kelvin effect (Hung and Hoffmann, 2015) to render S(IV) oxidation by O_2 on acidic microdroplets a potentially important pathway for heterogeneous sulfate production.

© Author(s) 2017. CC BY 4.0 License.

4 Conclusions

Our study suggests that both heterogeneous reactions (Case I and III-V) and in-cloud reactions (Case II) can dominate sulfate formation during Beijing haze. The $\Delta^{17}O$-constrained calculation shows that the heterogeneous sulfate production during haze events in our observation was mainly (66 to 73% on average) from reactions that result in sulfate with $\Delta^{17}O$=0‰, i.e., S(IV) oxidation by NO_2 and/or S(IV) oxidation by O_2 on acidic microdroplets. S(IV) oxidation by H_2O_2 and O_3 accounted for the rest (27 to 34%) of heterogeneous sulfate production. However, given the large difference in predicted aerosol pH assuming metastable aerosol state and stable aerosol state (pH = 7.6±0.1 and 4.7±1.1, respectively) and the strong dependence of S(IV) + NO_2 and S(IV) + O_2 on aerosol pH, we cannot quantify the relative importance of these two pathways for heterogeneous sulfate production. S(IV) + NO_2 in aerosol water can be the dominant pathway when aerosols are in stable state with pH = 7.6±0.1, while S(IV) + O_2 can take over providing that highly acidic aerosols (pH≤ 3) exist.To distinguish which of these two mechanisms is more important for sulfate formation during Beijing haze, the heterogeneity of aerosol state and pH should be considered in future studies.

Supplementary Materials

Table S1. Reaction rate expression and constant for SO_2 oxidation by OH in the gas-phase.
Table S2. The daytime average OH concentration.
Table S3. Aqueous-phase reaction rate expressions, rate constants (k) and influence of ionic strength (I_s) on k for sulfate production in aerosol and cloud water.
Table S4. The input and output of ISORROPIA II model.
Table S5. Calculations of aqueous-phase concentrations, equilibrium constants and influence of ionic strength.
Table S6. Observed $\Delta^{17}O(SO_4^{2-})$ in aerosols or rainwater in mid-latitude areas.

Data availability

All data needed to draw the conclusions in the present study are shown in this paper and/or the Supplementary Materials. For additional data related to this study, please contact the corresponding author (zqxie@ustc.edu.cn).

Author contributions

Z.Q.X. conceived and led the study. P.Z.H., X.Y.C, S.D.F., H.C.Z., H. K. performed the field experiments and aerosol chemical composition measurements. P.Z.H. conducted oxygen isotope measurements supervised by B.A. and L.G.. P.Z.H., B.A., Z.Q.X., L.G., H.S. and Y.F.C. interpreted the data. G.J.Z. involved the oxidation pathway calculation. C.L. contributed

© Author(s) 2017. CC BY 4.0 License.

to the field observation. P.Z.H. wrote the manuscript with B.A., Z.Q.X. and L.G. inputs and revision. All authors involved the discussion and revision.

Competing interests

The authors declare no competing interests.

Acknowledgments

We thank A. J. Schauer and Q. J. Chen at the University of Washington for help with isotope ratio measurements. Z.Q. Xie acknowledges support from National Key Project of MOST (2016YFC0203302), NSFC (91544013), and the Key Project of CAS (KJZD-EW-TZ-G06-01). B. Alexander acknowledges support from NSF AGS 1644998. H. Su acknowledges support from National Key Project of MOST (2017YFC0210104) and NSFC (91644218).

References

Alexander, B., Park, R. J., Jacob, D. J., and Gong, S.: Transition metal - catalyzed oxidation of atmospheric sulfur: Global implications for the sulfur budget, J. Geophys. Res., 114, D02309, 2009.

Alexander, B., Allman, D., Amos, H., Fairlie, T., Dachs, J., Hegg, D. A., and Sletten, R. S.: Isotopic constraints on the formation pathways of sulfate aerosol in the marine boundary layer of the subtropical northeast Atlantic Ocean, J. Geophys. Res., 117, D06304, 2012.

Bao, H., Thiemens, M. H., Farquhar, J., Campbell, D. A., Lee, C. C.-W., Heine, K., and Loope, D. B.: Anomalous 17O compositions in massive sulphate deposits on the Earth, Nature, 406, 176-178, 2000.

Bian, Y., Zhao, C., Ma, N., Chen, J., and Xu, W.: A study of aerosol liquid water content based on hygroscopicity measurements at high relative humidity in the North China Plain, Atmos. Chem. Phys., 14, 6417-6426, 2014.

Brook, R. D., Rajagopalan, S., Pope, C. A., Brook, J. R., Bhatnagar, A., Diez-Roux, A. V., Holguin, F., Hong, Y., Luepker, R. V., and Mittleman, M. A.: Particulate matter air pollution and cardiovascular disease an update to the scientific statement from the American Heart Association, Circulation, 121, 2331-2378, 2010.

Calhoun, J. A., Bates, T. S., and Charlson, R. J.: Sulfur isotope measurements of submicrometer sulfate aerosol particles over the Pacific Ocean, Geophys. Res. Lett., 18, 1877-1880, 1991.

Chen, Q., Schmidt, J. A., Shah, V., Jaeglé, L., Sherwen, T., and Alexander, B.: Sulfate production by reactive bromine: Implications for the global sulfur and reactive bromine budgets, Geophys. Res. Lett., 2017.

Cheng, Y., Zheng, G., Wei, C., Mu, Q., Zheng, B., Wang, Z., Gao, M., Zhang, Q., He, K., and Carmichael, G.: Reactive nitrogen chemistry in aerosol water as a source of sulfate during haze events in China, Sci. Adv., 2, e1601530, 2016.

© Author(s) 2017. CC BY 4.0 License.

425 Cheng, Z., Jiang, J., Fajardo, O., Wang, S., and Hao, J.: Characteristics and health impacts of particulate matter pollution in
426 China (2001–2011), Atmos. Environ., 65, 186-194, 2013.
427 Clifton, C. L., Altstein, N., and Huie, R. E.: Rate constant for the reaction of nitrogen dioxide with sulfur (IV) over the pH
428 range 5.3-13, Environ. Sci. Technol., 22, 586-589, 1988.
429 Dubey, M. K., Mohrschladt, R., Donahue, N. M., and Anderson, J. G.: Isotope specific kinetics of hydroxyl radical (OH)
430 with water (H2O): Testing models of reactivity and atmospheric fractionation, J. Phys. Chem. A, 101, 1494-1500, 1997.
431 Faloona, I.: Sulfur processing in the marine atmospheric boundary layer: A review and critical assessment of modeling
432 uncertainties, Atmos. Environ., 43, 2841-2854, 2009.
433 Feingold, G., Frost, G. J., and Ravishankara, A.: Role of NO3 in sulfate production in the wintertime northern latitudes, J.
434 Geophys. Res., 107, 2002.
435 Fountoukis, C., and Nenes, A.: ISORROPIA II: a computationally efficient thermodynamic equilibrium model for K+–
436 Ca2+–Mg2+–NH4+–Na+–SO42−–NO3−–Cl−–H2O aerosols, Atmos. Chem. Phys., 7, 4639-4659, 2007.
437 Fu, A.: Study on peroxides concentration and its influencing factors in the urban atmosphere, master of engineering, College
438 of Environmental and Resource Sciences, Zhejiang University, Hangzhou, China, 56 pp., 2014. (in Chinese)
439 Geng, L., Schauer, A. J., Kunasek, S. A., Sofen, E. D., Erbland, J., Savarino, J., Allman, D. J., Sletten, R. S., and Alexander,
440 B.: Analysis of oxygen - 17 excess of nitrate and sulfate at sub - micromole levels using the pyrolysis method, Rapid
441 Commun. Mass Spectrom., 27, 2411-2419, 2013.
442 Guo, H., Weber, R. J., and Nenes, A.: High levels of ammonia do not raise fine particle pH sufficiently to yield nitrogen
443 oxide-dominated sulfate production, Sci. Rep., 7, 12109, 2017.
444 Guo, J., Wang, Y., Shen, X., Wang, Z., Lee, T., Wang, X., Li, P., Sun, M., Collett, J. L., and Wang, W.: Characterization of
445 cloud water chemistry at Mount Tai, China: Seasonal variation, anthropogenic impact, and cloud processing, Atmos.
446 Environ., 60, 467-476, 2012.
447 Guo, S., Hu, M., Zamora, M. L., Peng, J., Shang, D., Zheng, J., Du, Z., Wu, Z., Shao, M., and Zeng, L.: Elucidating severe
448 urban haze formation in China, Proc. Natl Acad. Sci. USA., 111, 17373-17378, 2014.
449 Harris, E., Sinha, B., van Pinxteren, D., Tilgner, A., Fomba, K. W., Schneider, J., Roth, A., Gnauk, T., Fahlbusch, B., Mertes,
450 S., Lee, T., Collett, J., Foley, S., Borrmann, S., Hoppe, P., and Herrmann, H.: Enhanced Role of Transition Metal Ion
451 Catalysis During In-Cloud Oxidation of SO2, Science, 340, 727-730, 2013.
452 He, H., Wang, Y., Ma, Q., Ma, J., Chu, B., Ji, D., Tang, G., Liu, C., Zhang, H., and Hao, J.: Mineral dust and NOx promote
453 the conversion of SO2 to sulfate in heavy pollution days, Sci. Rep., 4, 4172, 2014.
454 Hennigan, C., Izumi, J., Sullivan, A., Weber, R., and Nenes, A.: A critical evaluation of proxy methods used to estimate the
455 acidity of atmospheric particles, Atmos. Chem. Phys, 15, 2775-2790, 2015.
456 Hoffmann, M. R., and Calvert, J. G.: Chemical Transformation Modules for Eulerian Acid Deposition Models: Volume II,
457 the Aqueous-phase Chemistry, Atmospheric Sciences Research Laboratory, Office of Research and Development, US
458 Environmental Protection Agency, 1985.

© Author(s) 2017. CC BY 4.0 License.

459 Holt, B., Kumar, R., and Cunningham, P.: Oxygen-18 study of the aqueous-phase oxidation of sulfur dioxide, Atmos.
460 Environ., 15, 557-566, 1981.
461 Hung, H.-M., and Hoffmann, M. R.: Oxidation of gas-Phase SO2 on the surfaces of acidic microdroplets: Implications for
462 sulfate and sulfate radical anion formation in the atmospheric liquid phase, Environ. Sci. Technol., 49, 13768-13776,
463 2015.
464 Ibusuki, T., and Takeuchi, K.: Sulfur dioxide oxidation by oxygen catalyzed by mixtures of manganese (II) and iron (III) in
465 aqueous solutions at environmental reaction conditions, Atmos. Environ., 21, 1555-1560, 1987.
466 Ishino, S., Hattori, S., Savarino, J., Jourdain, B., Preunkert, S., Legrand, M., Caillon, N., Barbero, A., Kuribayashi, K., and
467 Yoshida, N.: Seasonal variations of triple oxygen isotopic compositions of atmospheric sulfate, nitrate, and ozone at
468 Dumont d'Urville, coastal Antarctica, Atmos. Chem. Phys., 17, 3713-3727, 2017.
469 Jacob, D. J.: Heterogeneous chemistry and tropospheric ozone, Atmos. Environ., 34, 2131-2159, 2000.
470 Jenkins, K. A., and Bao, H.: Multiple oxygen and sulfur isotope compositions of atmospheric sulfate in Baton Rouge, LA,
471 USA, Atmos. Environ., 40, 4528-4537, 2006.
472 Jiang, J., Zhou, W., Cheng, Z., Wang, S., He, K., and Hao, J.: Particulate matter distributions in China during a winter period
473 with frequent pollution episodes (January 2013), Aerosol Air Qual. Res., 15, 494-503, 2015.
474 Lee, C. W., Savarino, J., Cachier, H., and Thiemens, M.: Sulfur (32S, 33S, 34S, 36S) and oxygen (16O, 17O, 18O) isotopic
475 ratios of primary sulfate produced from combustion processes, Tellus B, 54, 193-200, 2002.
476 Lee, Y. N., and Schwartz, S. E.: Kinetics of oxidation of aqueous sulfur (IV) by nitrogen dioxide, in: Kinetics of oxidation of
477 aqueous sulfur (IV) by nitrogen dioxide, Precipitation scavenging, dry Deposition and resuspension, California, 1982,
478 453-470, 1983.
479 Legrand, M., Hammer, C., De Angelis, M., Savarino, J., Delmas, R., Clausen, H., and Johnsen, S. J.: Sulfur ‐ containing
480 species (methanesulfonate and SO4) over the last climatic cycle in the Greenland Ice Core Project (central Greenland)
481 ice core, J. Geophys. Res., 102, 26663-26679, 1997.
482 Legrand, M., and Mayewski, P.: Glaciochemistry of polar ice cores: A review, Rev. Geophys., 35, 219-243, 1997.
483 Li, X., Bao, H., Gan, Y., Zhou, A., and Liu, Y.: Multiple oxygen and sulfur isotope compositions of secondary atmospheric
484 sulfate in a mega-city in central China, Atmos. Environ., 81, 591-599, 2013.
485 Liu, M., Song, Y., Zhou, T., Xu, Z., Yan, C., Zheng, M., Wu, Z., Hu, M., Wu, Y., and Zhu, T.: Fine Particle pH during
486 Severe Haze Episodes in Northern China, Geophys. Res. Lett., 2017.
487 Liu, X., and Millero, F. J.: The solubility of iron hydroxide in sodium chloride solutions, Geochim. Cosmochim. Acta, 63,
488 3487-3497, 1999.
489 Luz, B., and Barkan, E.: The isotopic ratios 17O/16O and 18O/16O in molecular oxygen and their significance in
490 biogeochemistry, Geochim. Cosmochim. Acta, 69, 1099-1110, 2005.
491 Matsuhisa, Y., Goldsmith, J. R., and Clayton, R. N.: Mechanisms of hydrothermal crystallization of quartz at 250 C and 15
492 kbar, Geochim. Cosmochim. Acta, 42, 173-182, 1978.

© Author(s) 2017. CC BY 4.0 License.

McArdle, J. V., and Hoffmann, M. R.: Kinetics and mechanism of the oxidation of aquated sulfur dioxide by hydrogen peroxide at low pH, J. Phys. Chem., 87, 5425-5429, 1983.

Meng, Z., Lin, W., Jiang, X., Yan, P., Wang, Y., Zhang, Y., Jia, X., and Yu, X.: Characteristics of atmospheric ammonia over Beijing, China, Atmos. Chem. Phys., 11, 6139-6151, 2011.

Rood, M., Shaw, M., Larson, T., and Covert, D.: Ubiquitous nature of ambient metastable aerosol, Nature, 337, 537-539, 1989.

Savarino, J., and Thiemens, M. H.: Analytical procedure to determine both δ18O and δ17O of H2O2 in natural water and first measurements, Atmos. Environ., 33, 3683-3690, 1999.

Savarino, J., Lee, C. C., and Thiemens, M. H.: Laboratory oxygen isotopic study of sulfur (IV) oxidation: Origin of the mass ‐ independent oxygen isotopic anomaly in atmospheric sulfates and sulfate mineral deposits on Earth, J. Geophys. Res., 105, 29079-29088, 2000.

Savarino, J., Alexander, B., Darmohusodo, V., and Thiemens, M. H.: Sulfur and oxygen isotope analysis of sulfate at micromole levels using a pyrolysis technique in a continuous flow system, Anal. Chem., 73, 4457-4462, 2001.

Seinfeld, J. H., and Pandis, S. N.: Atmospheric chemistry and physics: From air pollution to climate change, John Wiley & Sons, New Jersey, 2012.

Shen, C. H., and Rochelle, G. T.: Nitrogen dioxide absorption and sulfite oxidation in aqueous sulfite, Environ. Sci. Technol., 32, 1994-2003, 1998.

Shen, X., Lee, T., Guo, J., Wang, X., Li, P., Xu, P., Wang, Y., Ren, Y., Wang, W., and Wang, T.: Aqueous phase sulfate production in clouds in eastern China, Atmos. Environ., 62, 502-511, 2012.

Sun, Y., Zhuang, G., Tang, A., Wang, Y., and An, Z.: Chemical characteristics of PM2.5 and PM10 in haze-fog episodes in Beijing, Environ. Sci. Technol., 40, 3148-3155, 2006.

Vicars, W. C., and Savarino, J.: Quantitative constraints on the 17O-excess (Δ17O) signature of surface ozone: Ambient measurements from 50°N to 50°S using the nitrite-coated filter technique, Geochim. Cosmochim. Acta, 135, 270-287, 2014.

Walcek, C. J., and Taylor, G. R.: A theoretical method for computing vertical distributions of acidity and sulfate production within cumulus clouds, J. Atmos. Sci., 43, 339-355, 1986.

Wang, G., Zhang, R., Gomez, M. E., Yang, L., Zamora, M. L., Hu, M., Lin, Y., Peng, J., Guo, S., and Meng, J.: Persistent sulfate formation from London Fog to Chinese haze, Proc. Natl Acad. Sci. USA., 113, 13630-13635, 2016.

Wang, Y., Zhuang, G., Tang, A., Yuan, H., Sun, Y., Chen, S., and Zheng, A.: The ion chemistry and the source of PM2.5 aerosol in Beijing, Atmos. Environ., 39, 3771-3784, 2005.

Wang, Y., Zhang, Q., Jiang, J., Zhou, W., Wang, B., He, K., Duan, F., Zhang, Q., Philip, S., and Xie, Y.: Enhanced sulfate formation during China's severe winter haze episode in January 2013 missing from current models, J. Geophys. Res., 119, 10425-10440, 2014.

© Author(s) 2017. CC BY 4.0 License.

526 Ye, P., Xie, Z., Yu, J., and Kang, H.: Spatial distribution of methanesulphonic acid in the Arctic aerosol collected during the
527 Chinese Arctic Research Expedition, Atmosphere, 6, 699-712, 2015.
528 Zheng, B., Zhang, Q., Zhang, Y., He, K., Wang, K., Zheng, G., Duan, F., Ma, Y., and Kimoto, T.: Heterogeneous chemistry:
529 a mechanism missing in current models to explain secondary inorganic aerosol formation during the January 2013 haze
530 episode in North China, Atmos. Chem. Phys., 15, 2031-2049, 2015a.
531 Zheng, G., Duan, F., Su, H., Ma, Y., Cheng, Y., Zheng, B., Zhang, Q., Huang, T., Kimoto, T., and Chang, D.: Exploring the
532 severe winter haze in Beijing: the impact of synoptic weather, regional transport and heterogeneous reactions, Atmos.
533 Chem. Phys., 15, 2969-2983, 2015b.
534

535 **Figures and Tables**

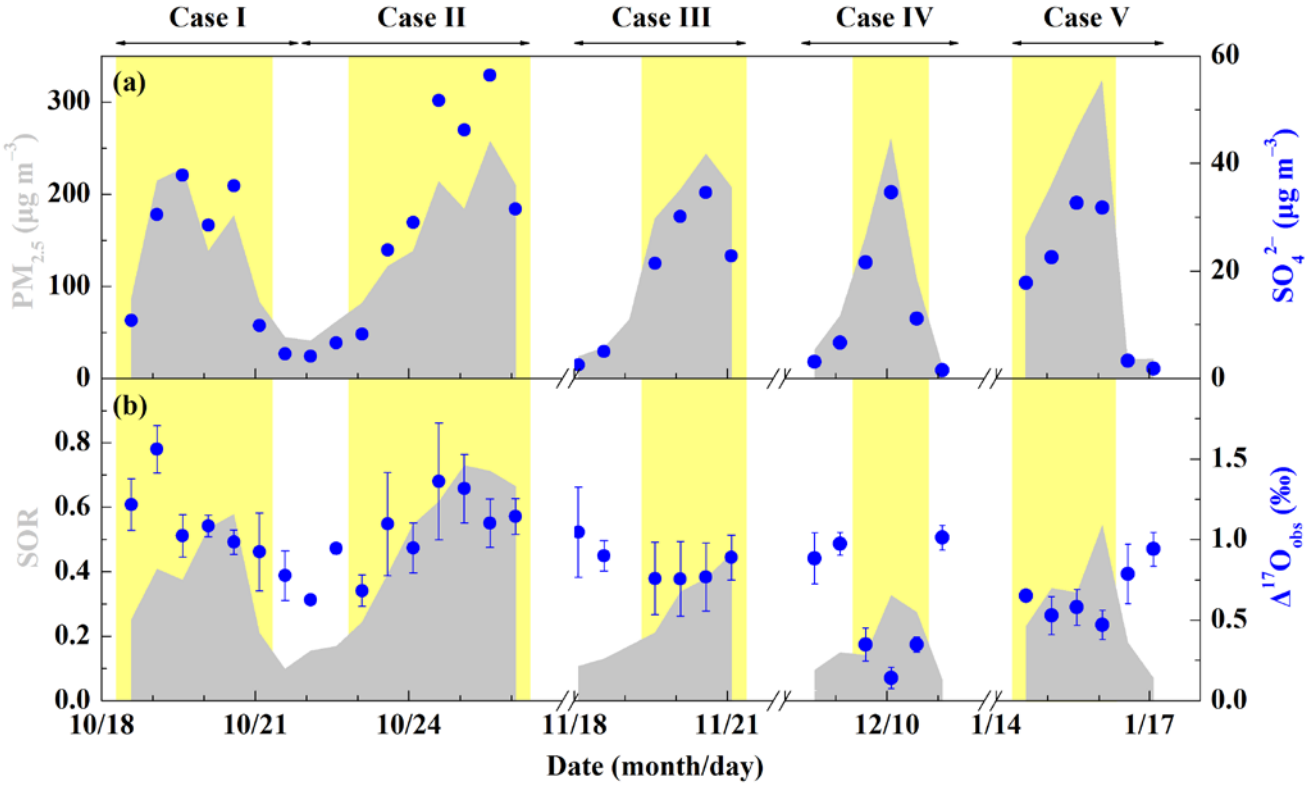

536

537 **Figure 1.** Characteristics of haze events in Beijing (October 2014–January 2015). **(a)** Temporal evolution of $PM_{2.5}$ and SO_4^{2-}
538 concentrations. **(b)**Temporal evolution of sulfur oxidation ratio (SOR = $nSO_4^{2-}/(nSO_4^{2-}+nSO_2)$, n represents the molar
539 concentration) and observed $\Delta^{17}O(SO_4^{2-})$ ($\Delta^{17}O_{obs}$). The error bar of $\Delta^{17}O_{obs}$in (b) is ±1σ of replicate measurements (n = 2–4)

© Author(s) 2017. CC BY 4.0 License.

of each sample. The light yellow shaded area indicates polluted days (PD, $PM_{2.5}\geq$ 75 μg m^{-3}). Data used here are 12h-averaged values, corresponding with filter samples.

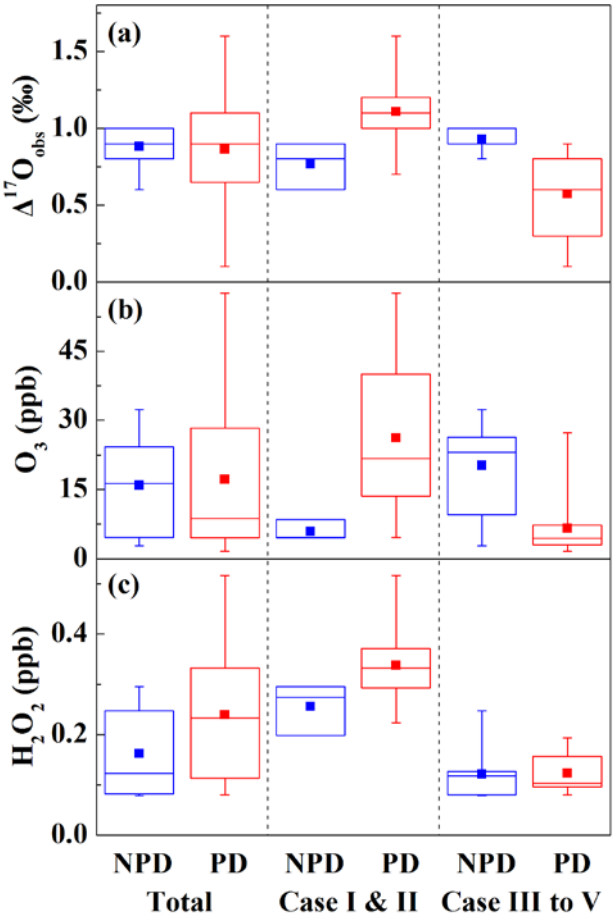

Figure 2. The box chart of observed $\Delta^{17}O(SO_4^{2-})$ ($\Delta^{17}O_{obs}$, **a**) and concentrations of observed O_3**(b)** and calculated H_2O_2**(c)** in non-polluted days (NPD, $PM_{2.5}<$ 75 μg m^{-3}) and polluted days (PD, $PM_{2.5}\geq$ 75 μg m^{-3}). The box line from bottom to top is respectively percentile of 25%, 50% and 75%, the whisker from bottom to top is respectively the minimum and the maximum, and the square is mean value.

Atmos. Chem. Phys. Discuss., https://doi.org/10.5194/acp-2017-977
Manuscript under review for journal Atmos. Chem. Phys.
Discussion started: 6 November 2017
© Author(s) 2017. CC BY 4.0 License.

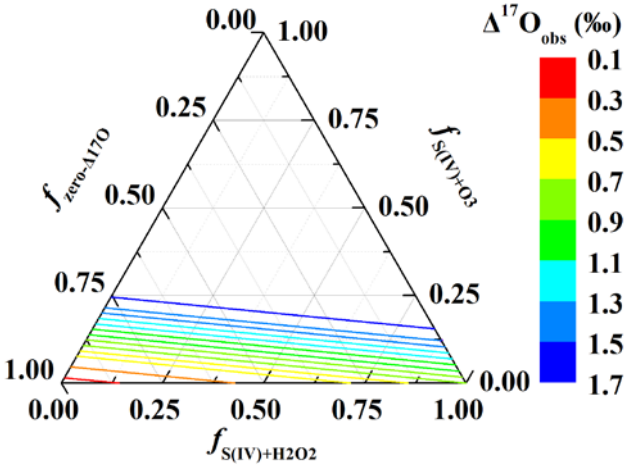

547

548 **Figure 3.** Ternary diagram of possible fractional contribution of different pathways to total sulfate production directly
549 estimated from $\Delta^{17}O_{obs}$.The colored lines are contour lines of $\Delta^{17}O_{obs}$, representing possible fractional contribution of sulfate
550 formation via O_3 ($f_{S(IV)+O3}$) and H_2O_2 ($f_{S(IV)+H2O2}$) oxidation or zero-$\Delta^{17}O$ processes ($f_{zero\text{-}\Delta17O}$) such as primary sulfate,
551 secondary sulfate formed via OH oxidation, NO_2 oxidation and O_2 oxidation initiated by TMIs in clouds or due to the
552 specialty of interfacial water on acidic microdroplets.

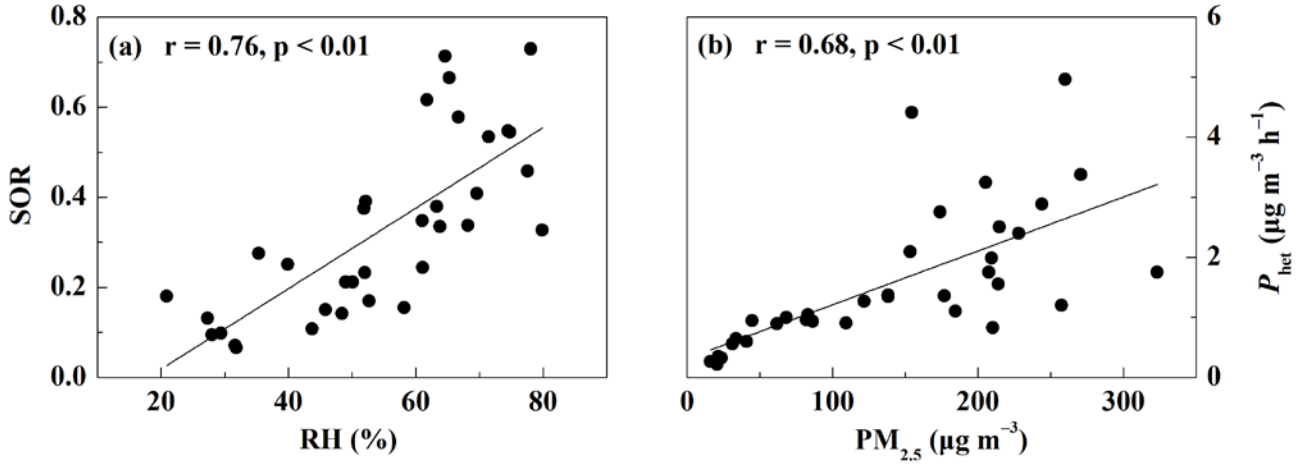

553

554 **Figure 4.** The relationship between RH and SOR **(a)** and relationship between $PM_{2.5}$ concentrations and rate of overall
555 heterogeneous sulfate production (P_{het}, **b**). The black lines are linear least-squares fitting lines.

Atmos. Chem. Phys. Discuss., https://doi.org/10.5194/acp-2017-977
Manuscript under review for journal Atmos. Chem. Phys.
Discussion started: 6 November 2017
© Author(s) 2017. CC BY 4.0 License.

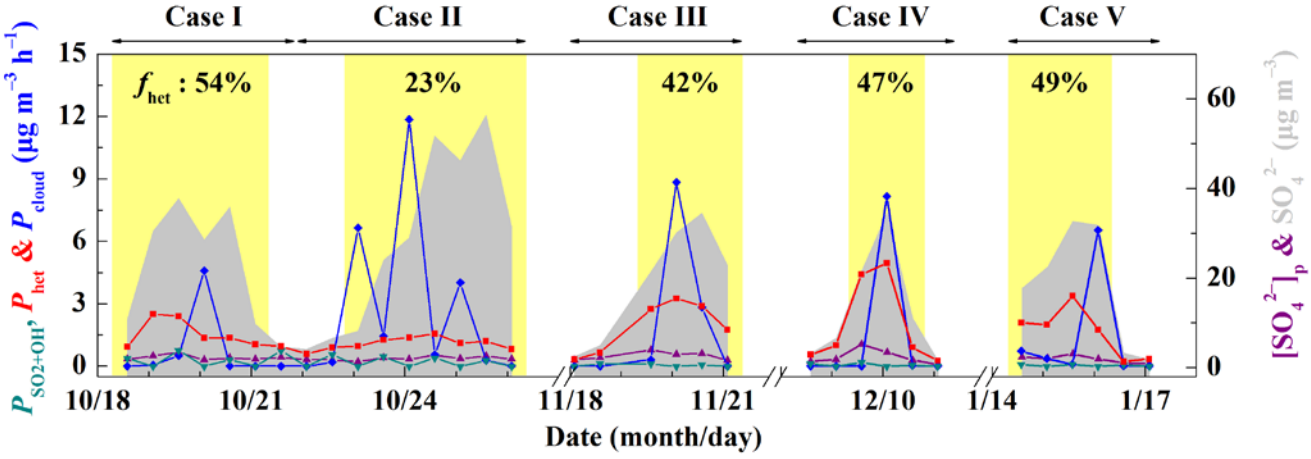

Figure5. Estimate of different sulfate production pathways. Time series of estimated sulfate production rate via OH oxidation in the gas-phase (P_{SO2+OH}), overall heterogeneous reactions on aerosols (P_{het}) and in-cloud reactions (P_{cloud}) and concentrations of primary sulfate ($[SO_4^{2-}]_p$) and observed sulfate. f_{het} represents the fraction of overall heterogeneous sulfate production to total sulfate production during PD of each Case. The light yellow shaded area indicates polluted days (PD, $PM_{2.5} \geq 75$ μg m^{-3}). Data used here are 12h-averaged values, corresponding with filter samples.

Atmos. Chem. Phys. Discuss., https://doi.org/10.5194/acp-2017-977
Manuscript under review for journal Atmos. Chem. Phys.
Discussion started: 6 November 2017
© Author(s) 2017. CC BY 4.0 License.

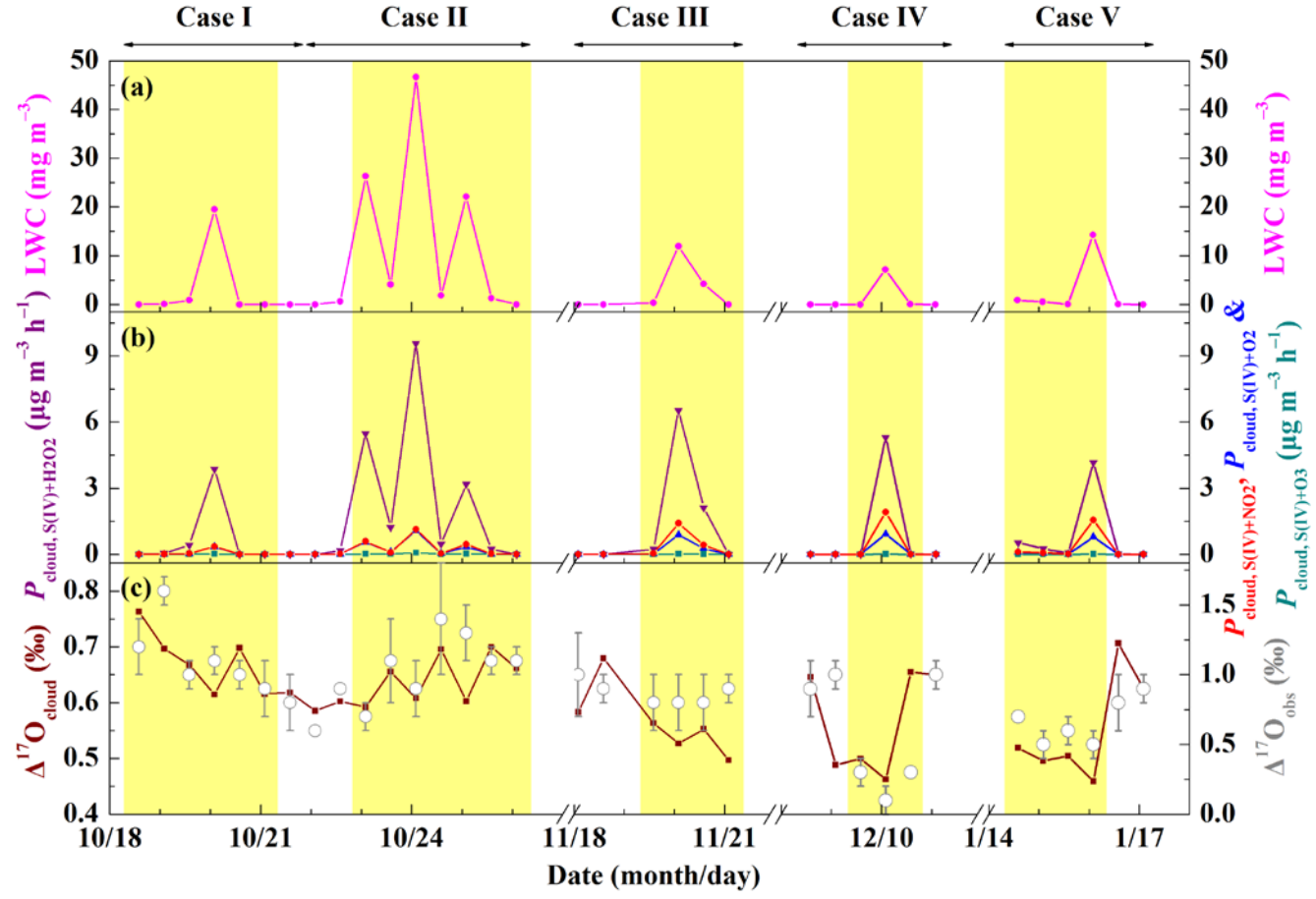

Figure 6. Temporal evolution of cloud liquid water content (LWC, **a**), in-cloud sulfate production rate via S(IV) oxidation by H_2O_2, O_3, NO_2 and O_2initiated by TMIs (denoted as $P_{cloud, S(IV)+H2O2}$, $P_{cloud, S(IV)+O3}$, $P_{cloud, S(IV)+NO2}$ and $P_{cloud, S(IV)+O2}$, respectively, **b**) and estimated $\Delta^{17}O$ of sulfate produced in clouds ($\Delta^{17}O_{cloud}$, **c**). The light yellow shaded area indicates polluted days (PD, $PM_{2.5} \geq 75$ μg m^{-3}). Data used here are 12h-averaged values, corresponding with filter samples.

Atmos. Chem. Phys. Discuss., https://doi.org/10.5194/acp-2017-977
Manuscript under review for journal Atmos. Chem. Phys.
Discussion started: 6 November 2017
© Author(s) 2017. CC BY 4.0 License.

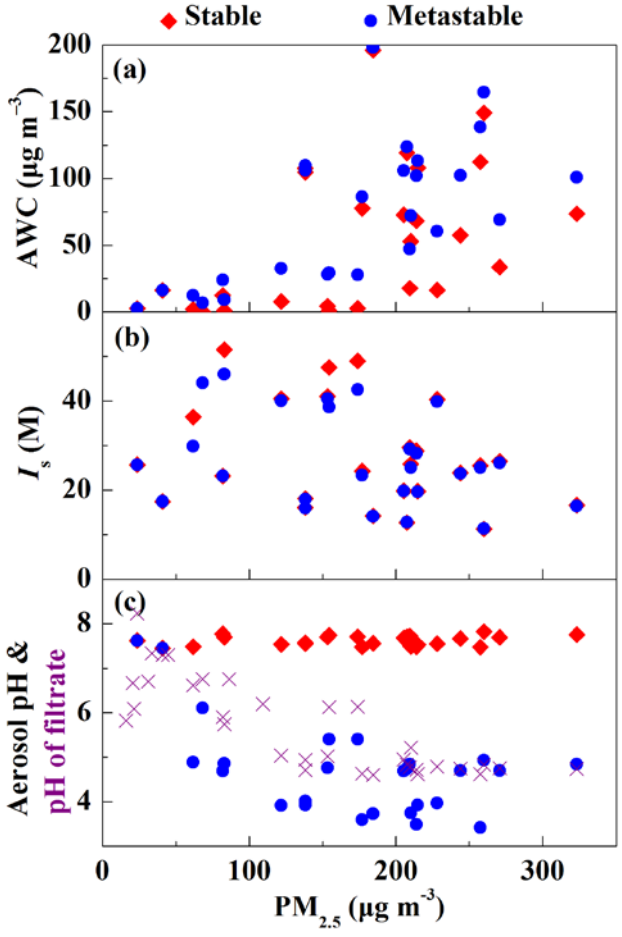

Figure 7. Aerosol parameters during Beijing haze. The aerosol water content (AWC, **a**), ionic strength (I_s, **b**) and aerosol pH (**c**) was predicted by ISORROPIA II assuming stable aerosol state and metastable aerosol state. The pH of filtrate was measured by an ion activity meter.

Atmos. Chem. Phys. Discuss., https://doi.org/10.5194/acp-2017-977
Manuscript under review for journal Atmos. Chem. Phys.
Discussion started: 6 November 2017
© Author(s) 2017. CC BY 4.0 License.

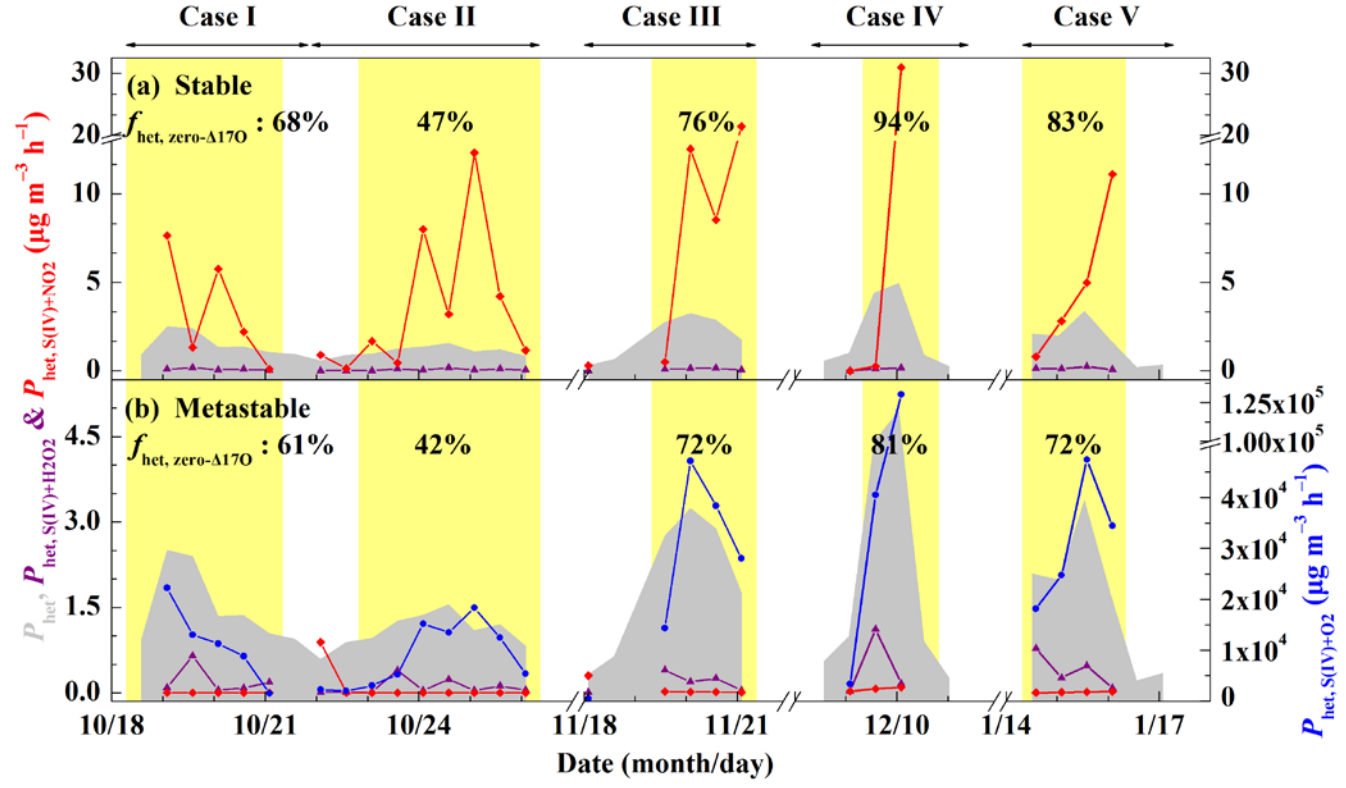

Figure8. Estimate of heterogeneous sulfate production pathways. Time series of overall heterogeneous sulfate production rate (P_{het}), heterogeneous sulfate production rate in aerosol water via H_2O_2 ($P_{het, S(IV)+H2O2}$) and NO_2 ($P_{het, S(IV)+NO2}$) under stable **(a)** and metastable **(b)** aerosol assumption. $P_{het, S(IV)+O2}$ in (b) represents heterogeneous sulfate production rate via SO_2 oxidation by O_2via a radical chain mechanisminitiated due to the specialty of interfacial water on acidic microdroplets. $f_{het, zero-\Delta17O}$ represents the fraction of heterogeneous reactions that result in sulfate with zero-$\Delta^{17}O$, such as S(IV) oxidation by NO_2 and O_2, to the overall heterogeneous sulfate production during PD of each Case with the constraint of $\Delta^{17}O(SO_4^{2-})$ (see the main text for details). In calculating $P_{het, S(IV)+H2O2}$, the influence of I_s was considered. In calculating $P_{het, S(IV)+NO2}$, and $P_{het, S(IV)+O2}$the influence of I_s was not considered due to the lack of experimental data about the influence of I_s. $P_{het, S(IV)+O2}$ was calculated using the aqueous-phase rate constant for pH ≤ 3 due to the lack of rate constant information at pH > 3. The light yellow shaded area indicates polluted days (PD, $PM_{2.5}$≥ 75 μg m^{-3}). Data used here are 12h-averaged values, corresponding with filter samples.

Atmos. Chem. Phys. Discuss., https://doi.org/10.5194/acp-2017-977
Manuscript under review for journal Atmos. Chem. Phys.
Discussion started: 6 November 2017
© Author(s) 2017. CC BY 4.0 License.

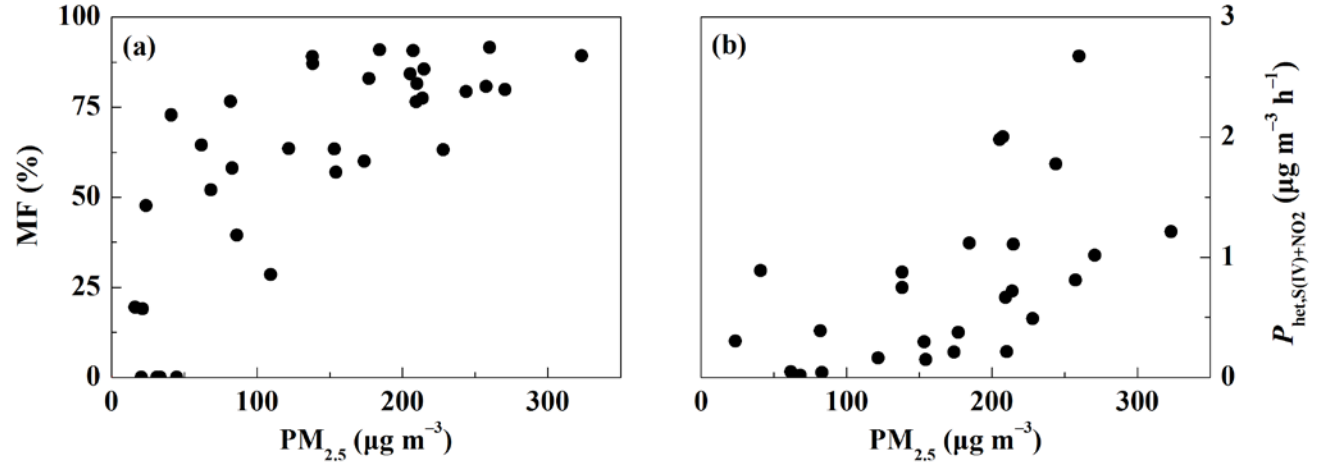

583

584 **Figure 9.** The estimated fraction of metastable aerosol to total aerosol (MF, **a**) using Eq. (9) and heterogeneous sulfate
585 production rate from S(IV) oxidation by NO_2 assuming a combination of metastable and stable state ($P_{het, S(IV)+NO2}$, **b**) as $P_{het, S(IV)+NO2} = MF \times P_{het, S(IV)+NO2, metastable} + (100\ \%–MF) \times P_{het, S(IV)+NO2, stable}$.

587

588 **Table 1.** Sulfate isotope assumptions.

Sulfate formation pathways	$\Delta^{17}O(SO_4^{2-})$ (‰)
SO_2 + OH	0
S(IV) + H_2O_2	0.7
S(IV) + O_3	6.5
S(IV) + NO_2	0
S(IV) + O_2	0
Primary sulfate	0

589